






A Technical-Economic Assessment of Producing Hydrogen and Biofuels via Gasification of Biomass in Solar Hybridised Dual Fluidised Bed

Nguyet K. Ngo¹ , Tara Hosseini² , Peter J. Ashman^{1,3,4} , Graham J. Nathan^{3,4,5} ,
and Woei L. Saw^{1,3,4} 

¹ School of Chemical Engineering, The University of Adelaide, SA 5005, Australia

² Commonwealth Scientific and Industrial Research Organization, CSIRO Energy, Australia

³ Heavy Industry, Low-carbon Transition Cooperative Research Centre

⁴ Centre for Energy Technology, The University of Adelaide, Australia

⁵ School of Electrical and Mechanical Engineering, The University of Adelaide, Australia

Abstract. This work assessed the techno-economic performances of three chemical conversion pathways using an upstream solar hybridised dual fluidised bed (SDFB) for biomass gasification. Using representative solar viability location in Australia with solar multiple ranges between 1.4-3.4 and thermal storage capacity designs with less than 1% solar dumping rate, the annual solar share varies between 7-17%, and the CO₂ emissions avoided relative to the non-solar case varies between 7%-23%. The projected break-even price varies between 5.5-6.1 AUD/kg (3.8-4.25 USD/kg) for hydrogen, 1.1-1.2 AUD/kg (0.75-0.85 USD/kg) for methanol, and 1.5-1.7 AUD/L (1.1-1.2 USD/L) for liquid fuels under the base case economic scenario. The derived break-even price from the SDFB gasifier configuration is higher than that of the non-solar counterpart, yet this depends on the supplementary heat supply and carbon credit.

Keywords: Solar-Hybridised Gasifier, CO₂ Mitigation, Biomass-to-Chemicals

1. Introduction

Solar-integrated biomass gasifier is a potential pathway for increasing biomass conversion efficiency into chemicals while decreasing emissions due to any combustion required for endothermic gasification process heating. Although this concept offers an option to chemically store the concentrated solar thermal (CST) energy, the intermittent solar resource remains a major challenge for continuous large-scale biofuel synthesis and hence accurate cost evaluation [1]. Several feasible options have been investigated to overcome the solar supply issue, such as CST energy storage in the form of syngas intermediate product, or transient operation control with indirectly irradiated reactors using an emissive plate [1], [2], [3], [4]. Previous studies indicated that the investment expense on heliostat mirrors, fuel cost, and environmental subsidies were key factors impacting the economic performance of the solar-integrated gasifiers [3], [4]. However, field size, fuel consumption, and renewable energy subsidies/credits are contingent upon the proportion of CST heat integrated into the process. Analysis of CST component designs, considering various associated costs or benefits scenarios, is necessary to determine the economic viability of hybridised solar-biomass gasifiers for biofuel/chemical synthesis and its future implications.

One feasible solution for solar-integrated biomass gasifiers is CST hybridisation with combustion back-up in directly irradiated reactors using a window. However, to maintain a nitrogen-free, hydrogen-rich syngas product stream, combustion should be separated from the gasification process. A solar hybridised dual fluidised bed (SDFB) gasifier configuration allows the steam gasification reaction without impurities from partial combustion, using inert solid particles as the fluidisation bed material and heat carrier from the CST unit or combustor to the gasifier [5]. This configuration decreases annual process emissions by partially replacing the sensible heat obtained from fuel combustion with CST energy while maintaining continuous syngas output [5]. Instead of storing syngas to maximize the utilization of CST energy, the concept offers an alternative of cheap and dense solid particles as a medium for thermal heat storage [5]. This introduces the concepts of solar multiple (SM), which defines the CST receiver oversized level to the nominal gasifier energy required, and storage capacity (SC) of the particle silo, which impacts the total SDFB gasifier operation hours under the CST-driven mode per annum. The SC design varies based on the SM and comes with capital expenditures for CST energy utilized, which selection impacts the overall cost-effectiveness. For this reason, both techno-economic analysis is required to obtain insights into the SM and SC selection for an SDFB gasifier.

Apart from solar integration, another approach for decarbonization involves capturing and compressing CO₂ for storage and utilization (CCUS). Pre-combustion CO₂ capture, integrated with the acid-gas-removal stage upstream of the biofuel synthesis [6], is a viable strategy. Several biofuel/ chemical productions are applicable from syngas, such as Hydrogen (H₂), Fischer Tropsch liquid fuels (TLFs), and Methanol (MeOH) [7], [8], with CO₂ capture being dependent on the target biofuel's carbon fraction. Meanwhile, solar integration into the SDFB gasifier stores carbon as biochar avoiding burning and being used for applications such as soil amendment [9]. These units' installation can be economically beneficial if credit is introduced for any CO₂ captured. Understanding the contribution of CO₂ mitigation from carbon capture and solar thermal techniques and its impact on economic viability is crucial for designing green biofuel synthesis processes. However, this understanding remains limited in the literature.

This study aims to conduct a preliminary technical-economic assessment of a stand-alone biofuel production plant utilizing H₂, MeOH, and TLFs from biomass via an SDFB gasifier, considering various combinations of SM and SC variables, alongside heat integration and sensitivity analysis on cost assumptions.

2. Methodology

Figure 1 shows the simplified process flow diagrams for three conversion routes. Aspen Plus simulation software was used for hourly heat and energy balance. A generic agricultural residue was used as the gasifier input. The typical meteorological year NatHERS 2016 files for Harwood-CZ0205, Australian climate zone were used to provide the DNI characteristics for the CST plant performance prediction. A biomass input scale of 150 MW_{th} to the SDFB gasifier was considered, based on modular scaling from an 8 MW_{th} dual fluidised bed (DFB) gasifier model [10] operating at 850°C atmospheric conditions. The solid separation unit was assumed to obtain a 90% char separation efficiency from sand through segregation.

The heliostat field was designed using CSIRO's Heliosim package. The direct normal solar irradiance (DNI_i) reflected from the heliostat mirror to the receiver at hour "i" was derived as $\dot{Q}_{solar,rec,i}$, and was determined based on the required steam gasification energy (\dot{Q}_{gasf} from Aspen model) as well as SM. Selected SM indicates the capacity of both solar heliostat field and receiver thus impacting the hourly $\dot{Q}_{DNI,i}$ and the total operation hours under CST-driven mode over the assessed time period. Energy loss through convection and re-radiation at hour "i" was considered for calculation of the hourly net useful energy directed to the storage silo, $\dot{Q}_{solar,net,i}$. The particle transportation energy losses (from the storage silos to the DFB gasifier) were assumed to be 5-10% [11]. Energy stored in the storage silo at t hour (\dot{Q}_{solar}) is the net

accumulation of the energy obtained from the hot particle storage silo $\dot{Q}_{solar,net,i}$ and the energy consumed by the gasification processes ($\dot{Q}_{gasf,i}$), based on the total hours under different SDFB operation modes. The material and energy flows of these modes were also plotted in **Figure 1**. Two operation modes were hourly selected based on the available storage silo CST energy (\dot{Q}_{solar}) and \dot{Q}_{gasf} .

$$\dot{Q}_{solar} = \sum_{i=1}^t [\dot{Q}_{solar,net,i} - \dot{Q}_{gasf,i} \times (1 + 10\%)] \quad (1)$$

- CST-driven mode:

$$If \frac{\dot{Q}_{solar}}{\dot{Q}_{gasf}} \geq 1: \dot{Q}_{gasf,i} = \dot{Q}_{gasf} \quad (2)$$

- DFB-combustor-driven mode:

$$If \frac{\dot{Q}_{solar}}{\dot{Q}_{gasf}} < 1: \dot{Q}_{gasf,i} = 0 \quad (3)$$

It was assumed that when \dot{Q}_{solar} reached its limit at hot particle silo storage capacity, the solar energy was dumped by defocusing the mirrors. This introduces the concept of solar dumping rate, which indicates the fraction of collected CST energy loss by spilling excess energy due to the selected operation strategy. Solar share (SS%), which identifies the fraction of CST distributed in total energy input (including CST input to the gasifier $\dot{Q}_{gasf,i}$, biomass input $\dot{Q}_{b,i}$, supplement fuel input $\dot{Q}_{sf,i}$) over the assessed period t , is another indicator of system performance.

$$SS\% = \frac{\sum_{i=1}^t \dot{Q}_{gasf,i}}{\sum_{i=1}^t \dot{Q}_{gasf,i} + \dot{Q}_{b,i} + \dot{Q}_{sf,i}} \quad (4)$$

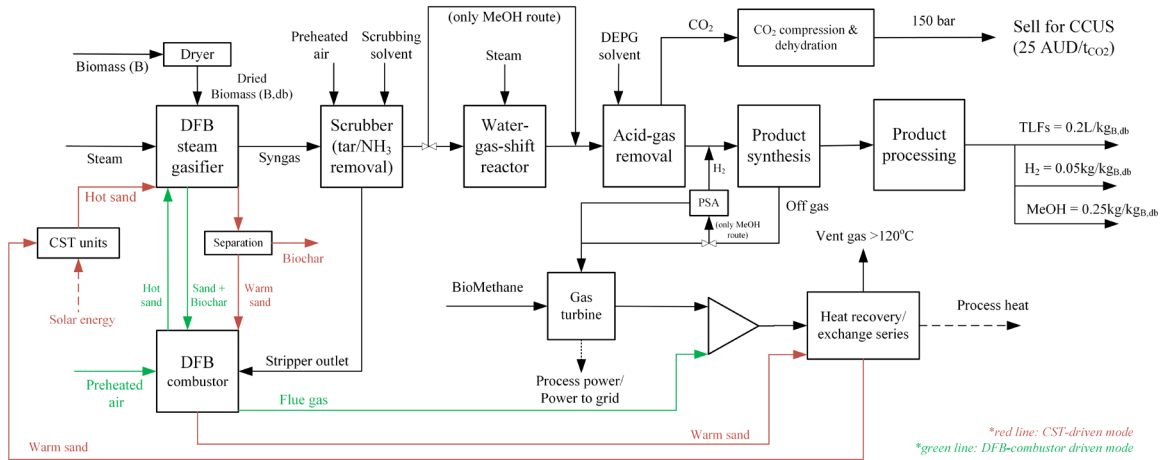


Figure 1. Block flow diagram showing base case configurations for three synthesis routes.

Raw syngas was configured to subsequently pass through a series of units to remove impurities and adjust the syngas compositions for different end-production routes. A PSA unit was used to separate hydrogen from the syngas, which can then be compressed for storage (H_2 route), recycled back to control the H_2/CO flowrate (MeOH route), or sent to a wax cracking unit to increase the diesel/gasoline production yield (TLFs route). The concentrated CO_2 stream captured from the dual-stage Selexol acid gas removal was assumed to pass through the CO_2 compression unit, in which supercritical CO_2 can be generated at 150 bar, ready for transportation, with the assumed power consumption rate of $230 \text{ kW}_e/t_{CO_2\text{-captured}}$ [12]. Off-gas exiting the biofuel production unit and any required supplemental fuel were sent to a downstream combined heat and power (CHP) cycle for self-sufficient operation. Turbine expander efficiency corresponding to each operation mode was assumed based on the ratio between part load and nominal operation flow rates. The air carrying tar from the oil-gas scrubber, along

with 10% uncovered biochar carried over by sand (separation unit recovery of 90%), were burnt in the DFB combustor. Recovered heat from the turbine and combustor was utilised by a series of heat exchangers. The model addressed transient heat supply variations resulting from the gasifier's CST-driven or DFB-combustor modes to meet the utility demand. A combination of solutions, such as adjusting the input stream flowrates of heat exchangers through mixing/ splitting the gas streams; using alternative heat exchangers for each operation mode; and using CST heat when feasible, were configured for the CHP cycle of each biofuel synthesis route. Exit gas was directed to a rotary dryer to remove moisture from biomass before vented.

Hourly DNI data was integrated with Aspen Plus data for different SM and SC designs to estimate annual system performance. The economic assessment used n^{th} -plant economics for a 30-year project lifetime with an 8.5% discount rate, assuming a 40%-60% equity-to-debt ratio, 3.7% interest rate, and 10-year debt maturity. Equipment costs were estimated using scaling methods, based on which the fixed capital investment (FCI), fixed operating cost (FOC) and total capital investment (TCI) were calculated following assumptions suggested in the literature [13], [14]. The CST component's costs were projected with linear scaling based on the cost per unit used in the previous study [14]. Direct production costs were assumed as follows: 0.2 AUD/GJ biomass, 15.2 AUD/GJ biomethane, 59.2 AUD/gal Selexol, 48 AUD/t silica, 0.3 AUD/m³ process water, 0.07 AUD/m³ cooling water. The utilities and solvent costs were estimated according to the first filling with an annual replacement of 1% top-up, while waste treatment was covered in TCI. Variable operating costs (VOC) include the total sum of direct production cost components as listed above, patents and royalties. Biochar was assumed to be sold for 1.1 AUD/kg for soil amendment application [9]. Credit on carbon sequestered in biochar was not considered for the base case scenario but assessed in the sensitivity analysis. The minimum selling price of products (denoted as MFSP) for each conversion route, ensuring net present value reaches zero at the plant's end, served as the economic indicator.

3. Results

3.1. CST component designs selected based on solar metrics

Figure 2 presents the two solar indicators as a function of SC for an SM of 3 using Harwood base case data for three conversion routes. The annual SS% increases in the order of H₂ < MeOH < TLFs route. This indicates the fraction of CST energy can be integrated into the process for the selected configurations. Given the same parameters assumed and hence the energy demand for driving the gasifier remains the same for all routes, this comparison shows that the CST energy required for downstream process heating is the highest for TLFs, while this value is lower for the other two routes. It is noted that the solar dumping rate, given the same CST storage duration for a fixed SM, remains unchanged for all routes.

Increasing the SM gives a higher annual SS%, so that the specific product output per biomass input is increased while the total CO₂ emissions avoided relative to the non-solar case also increases. For each SM, the critical SC capacity, defined as the point for which SS% starts to remain unchanged, should also be considered for better utilization of the CST energy with minimal cost. It can be seen from **Figure 2** that any SC beyond this point does not change the system performance. **Table 1** shows the capacity of the solar receiver and storage silos defined at its critical SC over the studied SM range which gives approximately a 1% dumping rate. Although from the environmental perspective, a higher SM with its critical SC is preferred, economic feasibility is another criterion to be considered for CST component designs.

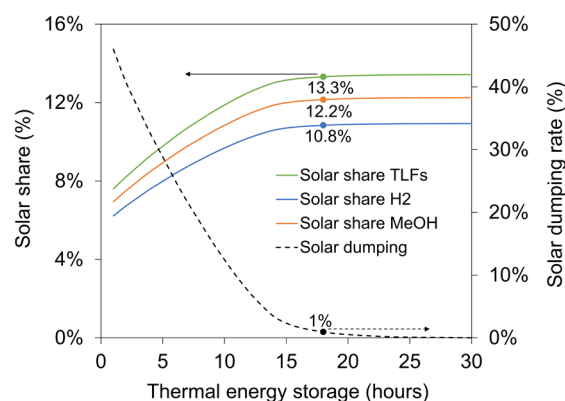


Figure 2. The dependence of annual SS% and dumping rate on SC at SM of 3.

Table 1. The capacity of CST unit components as a function of SM and SC for 150 MW_{th} gasifier input.

SM	MeOH route receiver (MW _{th})	H ₂ route receiver (MW _{th})	TLFs route receiver (MW _{th})	SC (hours)	MeOH route storage (MWh _{th})	H ₂ route storage (MWh _{th})	TLFs route storage (MWh _{th})
1.4	37	36	42	2.5	59	58	67
1.8	48	46	53	5.5	131	127	147
2.2	58	56	65	9.0	214	207	241
2.6	69	67	77	12.5	297	288	334
3.0	79	77	89	17.5	416	403	468
3.4	90	87	101	37.0	892	852	990

3.2. Energy efficiency and CO₂ mitigation

Figure 3 presents the LHV energy conversion and CO₂ emissions (denoted as CO_{2-e}) for three conversion routes. For H₂ production, the energetic conversion efficiency ranges between 28.5%-32% for the assessed SDFB gasifier scenario as shown in Table 1. These figures are slightly lower for MeOH and TLFs, fluctuating between 24%-28.5%. Two additional scenarios were compared here. Scenario X1, which was configured with neither CCS nor CST unit installation, yields efficiencies of 38% for H₂, 32.5% for MeOH, 31% for TLFs; and Scenario X2, configured with CCS but without solar integration, projecting efficiencies 1-2% lower than X1. The SDFB cases' low efficiency is mainly due to the annual accumulated heat losses associated with CST components, amounting to 60% of the energy collected from the heliostat field. However, when considering only useful CST energy ($\sum_{i=1}^t [\dot{Q}_{gasf,i}]$) and excluding losses by CST components, the efficiency range improves to 31%-38%. Energy losses due to part-load operation of the turbine or waste heat discharged from the downstream transient CHP cycle are other factors with minor effects.

The projected CO₂ emissions rate increases in the order of MeOH < TLFs < H₂ for the assessed configurations without considering the utilization of any CO₂ mitigation approach (X1). Among the three conversion routes, the largest CO₂ discharged volume is obtained from H₂ synthesis as carbon needs to be removed from the final product. However, with CCS installed to the CO₂ captured from the Selexol unit (X2), despite the slightly lower efficiency, the CO₂ emissions rate is reduced dramatically by 26 wt.% for H₂ production route. With CST integration, the annual average CO₂ emissions over the assessed SM range was 1.12-1.26 t_{CO2-e}/t_{biomass,db}, compared to 1.35 for scenario X2 or 1.82 for scenario X1. For the MeOH route, the amount of CO₂ captured is limited by the component fractions required for product synthesis, which is equivalent to an emissions rate of 0.13 t_{CO2-e}/t_{biomass,db} or 9% CO₂ reduction compared to that of scenario X1. Meanwhile, these figures for TLFs synthesis are projected to be 0.2 t_{CO2-e}/t_{biomass,db} and 14%, respectively. With CST integration, the projected CO₂ emissions rates for these two routes vary between 0.95 and 1.13 t_{CO2-e}/t_{biomass,db} over the assessed SM

range. This is equivalent to a further 8%-20% reduction in CO₂ emissions, on top of that can be mitigated in scenario X2. It is noted that the biofuel production capacity remains unchanged in these comparisons, and the CO₂ mitigation due to CST integration is contributed mainly by the supplement fuel saved and biochar not being burnt. It can be seen that for a fixed solar oversize (i.e. SM=3), the contribution to CO₂ mitigation due to CST energy integration is less than half compared to pre-combustion CO₂ capture for H₂ synthesis. However, its contribution becomes more significant for TLFs and nearly doubles for MeOH synthesis routes.

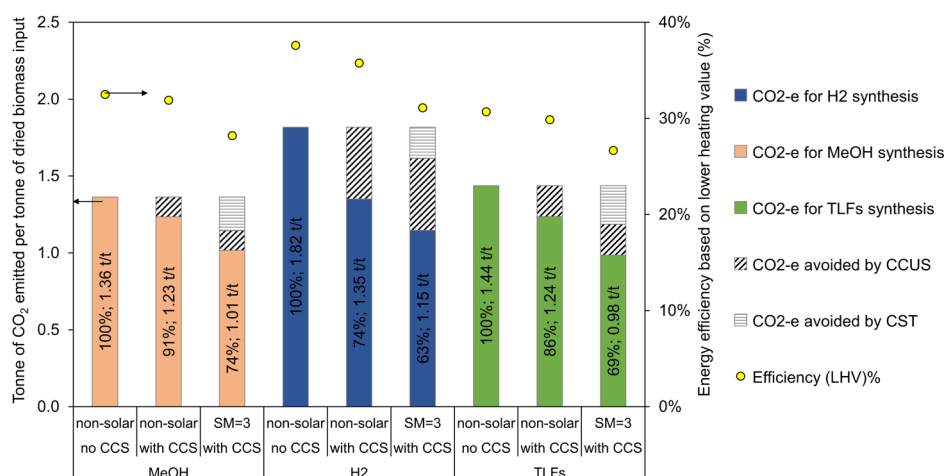


Figure 3. Comparison on CO₂ emissions and energy efficiency of three base case scenarios with scenarios X1 and X2.

3.3. Economic viability

Figure 4 presents the MFSP cost breakdown of assessed scenarios using both non-solar and SDFB gasifiers with an SM = 3, 17.5 hours storage. Figure 5 presents the MFSP of different product synthesis configurations under different economic assumptions of fuel cost and CO₂ credit. Under the base case assumptions, the calculated MFSP of MeOH is 1.1 AUD/kg (0.8 USD/kg using an exchange rate of 1 AUD₂₀₂₂ = 0.695 USD₂₀₂₂) for the non-solar scenario X2, and 1.1-1.2 AUD/kg (or 0.75-0.85 USD/kg) for CST-integrated scenario over the assessed designs. This is nearly double the high-end 2018-2021 global MeOH spot price of 0.45 USD/kg. The projected MFSP of H₂ is 5.5 AUD/kg (3.8 USD/kg) for the non-solar scenario, and 5.7-6.1 AUD/kg (3.95-4.25 USD/kg) for the assessed CST scenario. Although considerably higher than the 2050 green H₂ target price of 1.5-2.0 USD/kg, this cost aligns with estimates for other net-zero H₂ synthesis pathways [4], [15]. The high projected price is also influenced by the volume and cost of the supplemental fuel required for providing process thermal heat during DFB-combustion operation mode. The base case MFSP of TLFs is calculated to be 1.5 AUD/L (1.05 USD/L) for the non-solar scenario and is approximately 1.6-1.7 AUD/L (1.1-1.2 USD/L) over the assessed CST designs. These projections closely match wholesale TLFs prices with the least deviation among the three routes.

Figure 4 indicates that the capital investment dominates the “costs” components of MFSP with CST unit significantly impacting total expense, depending on the configured SS%. This additional CST investment is the main reason for the 3%-5% higher MFSP calculated for the CST-integrated scenarios (SM=1.4-3) relative to the non-solar case. Higher SM (3.4) leads to a sharper increase of MFSP by 10%, due to the high capital expense associated with the long solar storage duration required for the same utilization level of collected CST energy which is beyond the 24-hour day. However, if the cost of the supplement fuel rises or additional carbon credit is factored in for CO₂ mitigation, this accumulated benefit will increase, altering its relationship with CST capital cost, as shown in Figure 5. The MFSP discrepancy between non-solar and CST-integrated scenarios diminishes with higher biomethane costs until it reaches a point where solar cases become more viable. Indeed, this supplemental heat can be a biomass

fuel or green power depending on the configurations selected for the utility demands. At a high-end biomethane cost of 30 AUD/GJ (21 USD/GJ), the MFSP of MeOH determined at an SM range of 1.8-3 and TLFs at an SM of 2.2-3 becomes competitive with a non-solar system, however, not for the H₂ route. For the H₂ route, further optimization on CHP configurations can be done to replace this biomethane with a cheaper, low-grade energy source, considering transient upstream operation. Similarly, the relationship between CST investment and solar operating benefits is also influenced by environmental subsidies, such as claiming a carbon credit on biochar. To render the SDFB gasifier competitive with the non-solar case, the required threshold for this carbon credit increases in the order of MeOH < TLFs < H₂, defined at 80-95 AUD/t_{CO2} (56-66 USD/t_{CO2}), typically near a SM of 2.6-3 under these conditions.

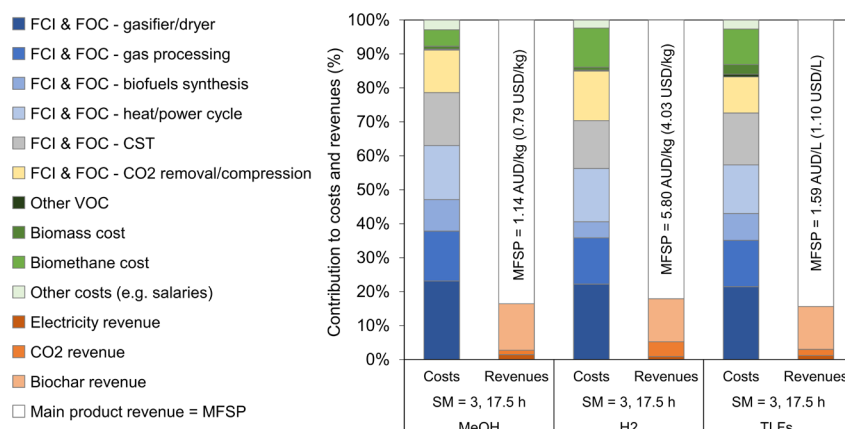


Figure 4. Base case MFSP breakdown.

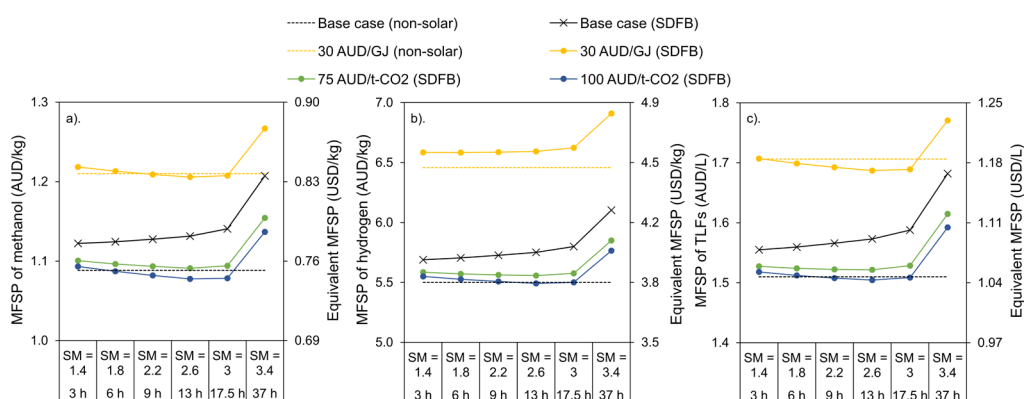


Figure 5. The MFSP calculated for a) methanol, b) hydrogen, c) TLFs under different assumptions.

4. Conclusions

A TEA of H₂, MeOH and TLFs synthesis from an SDFB gasifier was conducted to assess the impact of different economic assumptions on overall performance, as a function of CST component designs. The integration of CST energy reduces the process CO₂ emissions by 7-9% (at SM = 1.4) to 17-23% (at SM = 3.4); however, it also leads to a reduction in energy efficiency due to CST heat losses. The impact on CO₂ reduction by CST integration is less significant than pre-combustion CO₂ capture for H₂ synthesis but becomes more significant for other production routes. The estimated biofuel MFSPs are higher than the current market and that projected for conventional DFB gasifier configuration. However, there is a potential competitiveness for the proposed SDFB gasifier with its non-solar counterpart, which can be achieved at an elevated green fuel cost (21 USD/GJ for TLFs/ MeOH) or the introduction of a (biochar) carbon storage credit (56 USD/t_{CO2} for TLFs/ MeOH and 66 USD/t_{CO2} for H₂).

Data availability statement

Data can be made available upon request.

Underlying and related material

Relevant studies on techno-economic evaluation of solar-hybridised dual fluidised bed (SDFB) gasifier: <https://doi.org/10.1021/acs.energyfuels.3c04329>.

Author contributions

Nguyet K. Ngo: conceptualization, methodology, formal analysis, original draft, **Woei L. Saw:** conceptualization, review & editing, **Tara Hosseini:** conceptualization, methodology, **Peter J. Ashman:** conceptualization, **Graham J. Nathan:** conceptualization.

Competing interests

The authors declare that they have no competing interests.

Funding

This work is funded by the Future Fuels CRC, supported through the Australian Government's Cooperative Research Centres Program. We gratefully acknowledge the cash and in-kind support from all our research, government and industry participants.

References

- [1] Saw, W.L., P. Guo, P.J. van Eyk, and G.J. Nathan, "Approaches to accommodate resource variability in the modelling of solar driven gasification processes for liquid fuels synthesis", *Solar Energy*, vol. 156, pp. 101-112, 2017, doi: <https://doi.org/10.1016/j.solener.2017.05.085>.
- [2] Rahbari, A., A. Shirazi, M.B. Venkataraman, and J. Pye, "A solar fuel plant via supercritical water gasification integrated with Fischer–Tropsch synthesis: Steady-state modelling and techno-economic assessment", *Energy Conversion and Management*, vol. 184, pp. 636-648, 2019, doi: <https://doi.org/10.1016/j.enconman.2019.01.033>.
- [3] Bai, Z., Q. Liu, L. Gong, and J. Lei, "Investigation of a solar-biomass gasification system with the production of methanol and electricity: Thermodynamic, economic and off-design operation", *Applied Energy*, vol. 243, pp. 91-101, 2019, doi: <https://doi.org/10.1016/j.apenergy.2019.03.132>.
- [4] Boujjat, H., S. Rodat, and S. Abanades, "Techno-Economic Assessment of Solar-Driven Steam Gasification of Biomass for Large-Scale Hydrogen Production", *Processes*, vol. 9, pp. 462, 2021, doi: <https://doi.org/10.3390/pr9030462>.
- [5] Guo, P., P.J. Van Eyk, W.L. Saw, P.J. Ashman, G.J. Nathan, and E.B. Stechel, "Performance assessment of Fischer–Tropsch liquid fuels production by solar hybridized dual fluidized bed gasification of lignite", *Energy & Fuels*, vol. 29, pp. 2738-2751, 2015, doi: <https://doi.org/10.1021/acs.energyfuels.5b00007>.
- [6] Jansen, D., M. Gazzani, G. Manzolini, E. van Dijk, and M. Carbo, "Pre-combustion CO₂ capture", *International Journal of Greenhouse Gas Control*, vol. 40, pp. 167-187, 2015, doi: <https://doi.org/10.1016/j.ijggc.2015.05.028>.
- [7] Jeevahan, J., A. Anderson, V. Sriram, R. Durairaj, G. Britto Joseph, and G. Mageshwaran, "Waste into energy conversion technologies and conversion of food wastes into the potential products: a review", *International Journal of Ambient Energy*, pp. 1-19, 2018, doi: <https://doi.org/10.1080/01430750.2018.1537939>

- [8] Ciferno, J.P. and J.J. Marano, "Benchmarking biomass gasification technologies for fuels, chemicals and hydrogen production.", 2002. <https://www.netl.doe.gov/sites/default/files/netl-file/BMassGasFinal.pdf>.
- [9] Campbell, R.M., N.M. Anderson, D.E. Daugaard, and H.T. Naughton, "Financial viability of biofuel and biochar production from forest biomass in the face of market price volatility and uncertainty", *Applied Energy*, vol. 230, pp. 330-343, 2018, doi: <https://doi.org/10.1016/j.apenergy.2018.08.085>.
- [10] Kraft, S., F. Kirnbauer, and H. Hofbauer, "CPFD simulations of an industrial-sized dual fluidized bed steam gasification system of biomass with 8 MW fuel input", *Applied Energy*, vol. 190, pp. 408-420, 2017, doi: <https://doi.org/10.1016/j.apenergy.2016.12.113>.
- [11] ASTRI, "Details of 120 Mwe Molten Salt Central Receiver Plant with SCO₂ Power Block", (internal report), 2014.
- [12] Aspelund, A. and K. Jordal, "Gas conditioning—The interface between CO₂ capture and transport", *International Journal of Greenhouse Gas Control*, vol. 1, pp. 343-354, 2007, doi: [https://doi.org/10.1016/S1750-5836\(07\)00040-0](https://doi.org/10.1016/S1750-5836(07)00040-0).
- [13] Peters, M.S., K.D. Timmerhaus, and R.E. West, "Plant design and economics for chemical engineers", 5th ed., New York: McGraw-Hill, 2003.
- [14] Ngo, N.K., Smith, T., Nathan, G., Ashman, P., Hosseini, T., Beath, A., Stechel, E.B., and Saw, W.L., "Techno-Economic Evaluation of Solar Hybridized Biomass Gasification Polygeneration Plants", *Energy & Fuels*, vol. 38, pp. 2058-2073, 2024, doi: <https://doi.org/10.1021/acs.energyfuels.3c04329>.
- [15] Longden, T., F.J. Beck, F. Jotzo, R. Andrews, and M. Prasad, "'Clean' hydrogen?—Comparing the emissions and costs of fossil fuel versus renewable electricity based hydrogen", *Applied Energy*, vol. 306, pp. 118-145, 2022, doi: <https://doi.org/10.1016/j.apenergy.2021.118145>.